SETD2 regulates SLC family transporter-mediated sodium and glucose reabsorptions in renal tubule

Taku Mitome
Yokohama City University Graduate School of Medicine
Hiromichi Wakui
Yokohama City University Graduate School of Medicine
Kengo Azushima
Yokohama City University Graduate School of Medicine
Tatsuki Uehara
Yokohama City University Graduate School of Medicine
Ryosuke Jikuya
Yokohama City University Graduate School of Medicine
Shinji Ohtake
Yokohama City University Graduate School of Medicine
Go Noguchi
Yokohama City University Graduate School of Medicine
Sachi Kawaura
Yokohama City University Graduate School of Medicine
Yasuhiro Iribe
Yokohama City University Graduate School of Medicine
Kota Aomori
Yokohama City University Graduate School of Medicine
Tomoyuki Tatenuma
Yokohama City University Graduate School of Medicine
Hiroki Ito
Yokohama City University Graduate School of Medicine
Takashi Kawahara
Yokohama City University Graduate School of Medicine
Mitsuru Komeya
Yokohama City University Graduate School of Medicine
Yusuke Ito
Yokohama City University Graduate School of Medicine
Kentaro Muraoka
Yokohama City University Graduate School of Medicine
Mitsuko Furuya

Eurofins Genetic Lab Co., Ltd

Ikuma Kato
Yokohama City University Graduate School of Medicine

Satoshi Fujii
Yokohama City University Graduate School of Medicine

Kiyotaka Nagahama
Kyorin University

Akira Nishiyama
Yokohama City University Graduate School of Medicine

Tomohiko Tamura
Yokohama City University Graduate School of Medicine

Yayoi Kimura
Yokohama City University Graduate School of Medicine

Tatsukata Kawagoe
Yokohama City University Graduate School of Medicine

Nobuhisa Mizuki
Yokohama City University Graduate School of Medicine

Gang Huang
Cincinnati Children's Hospital Medical Center

Hiroji Uemura
Yokohama City University Graduate School of Medicine

Masahiro Yao
Yokohama City University Graduate School of Medicine

Kazuhide Makiyama
Yokohama City University Graduate School of Medicine

Kouichi Tamura
Yokohama City University Graduate School of Medicine

Hisashi Hasumi
hasumi@yokohama-cu.ac.jp

Yokohama City University Graduate School of Medicine

Article

Keywords: SETD2, SLC family transporter, Diabetes mellitus, Cardiovascular diseases, Hypertension, Kidney cancer

Posted Date: March 28th, 2024

DOI: https://doi.org/10.21203/rs.3.rs-4019251/v1

Additional Declarations: No competing interests reported.

Abstract

A regulatory mechanism for SLC family transporters, critical transporters for sodium and glucose reabsorptions in renal tubule, is incompletely understood. Here, we report an important regulation of SLC family transporter by *SETD2*, a chromatin remodeling gene whose alterations have been found in a subset of kidney cancers. Kidney-specific inactivation of *Setd2* resulted in hypovolemia with excessive urine excretion in mouse and interestingly, RNA-sequencing analysis of *Setd2*-deficient murine kidney exhibited decreased expressions of SLC family transporters, critical transporters for sodium and glucose reabsorptions in renal tubule. Importantly, inactivation of *Setd2* in murine kidney displayed attenuated dapagliflozin-induced diuresis and glucose excretion, further supporting that *SETD2* might regulate SLC family transporter-mediated sodium and glucose reabsorptions in renal tubule. These data uncover an important regulation of SLC family transporter by *SETD2*, which may illuminate a crosstalk between metabolism and epigenome in renal tubule.

Introduction

SET domain-containing 2 (SETD2) is the primary methyltransferase for histone 3 lysine-36 trimethylation (H3K36me3) and *SETD2*-mediated H3K36me3 is involved in the regulation of alternative splicing, mRNA methylation, and DNA mismatch repair in mammalian cells [1,2]. *SETD2* has been shown as one of important tumor suppressors in a variety of cancers and of note, *SETD2* has been reported to play an important role in renal tumor suppression since variants in *SETD2* have been found in a subset of kidney cancers, and inactivation of *SETD2* in a *c-MYC*–driven polycystic kidney disease (PKD) mouse model lead to the development of clear cell renal cell carcinoma [3–5].

To elucidate physiological roles for *SETD2* in renal tubule, we developed kidney-specific *Setd2* knockout mouse model and analyzed this mouse model using metabolic chamber. We also conducted RNA sequencing analysis to decipher an underlying mechanism for the phenotypes observed in *Setd2*-deficienty kidney. To further validate those results, we performed pharmacological stress tests using a variety of inhibitors for renal tubule transporters.

Results

Kidney-specific inactivation of Setd2 leads to hypovolemia with renal dysfunction in mouse.

To explore a physiological role for *SETD2* in renal tubule, we inactivated *Setd2* specifically in mouse kidney using *PAX8-Cre* transgenic mouse and confirmed the inactivation of *Setd2* as well as the downregulation of histone H3 trimethylation at lysine 36 (H3K36me3) in *Setd2*-deficient kidney (Fig. 1A). Although kidney to body weight ratio was lower in kidney-specific *Setd2* knockout mouse compared to that in control mouse, histological alterations were not observed in *Setd2*-deficient kidney (Fig. 1B and C). Interestingly, kidney-specific *Setd2* knockout mouse exhibited decreased blood pressure with elevated

serum creatinine (CRE) and blood urea nitrogen (BUN), suggesting that inactivation of *Setd2* in mouse kidney might lead to hypovolemia with renal dysfunction (Fig. 1D and E).

Kidney-specific inactivation of Setd2 leads to defective urinary concertation in mouse.

To clarify how kidney-specific inactivation of *Setd2* leads to hypovolemia, we analyzed kidney-specific *Setd2* knockout mouse using metabolic chamber. Interestingly, kidney-specific *Setd2* knockout mouse showed increased urine volume with increased water intake (Fig. 2A). Next, we conducted water restriction test and found that kidney-specific *Setd2* knockout mouse lost more weight after water restriction for twenty-four hours (Fig. 2B). Importantly, kidney-specific *Setd2* knockout mouse exhibited decreased urinary osmolality (Uosm) as well as increased plasma osmolality (Posm) after water restriction for twenty-four hours, suggesting that kidney-specific *Setd2* knockout mouse might have a defect in urinary concentration (Fig. 2B).

Kidney-specific inactivation of Setd2 leads to decreased expression of SLC family transporters.

To decipher an underlying mechanism how kidney-specific inactivation of *Setd2* lead to defective urinary concentration, we performed RNA sequencing of *Setd2*-deficient kidney. Intriguingly, Reactome Pathway analysis of RNA sequencing data exhibited the downregulation of solute carrier (SLC) family-mediated membranous transport pathway in *Setd2*-deificient kidney (Fig. 3A). Indeed, expressions of *Slc9a3/Nhe3, Slc5a2/Sglt2* and *Slc12a1/Nkcc2*, important SLC family transporters in renal tubules, were decreased in *Setd2*-deificient kidney, suggesting that defective urinary concentration in *Setd2*-deficient kidney may be due to dysregulated SLC family transporters (Fig. 3B).

Setd2 -deficient kidney exhibits attenuated dapagliflozin-induced diuresis and glucose excretion.

To further examine the function of SLC family transporters in *Sedt2*-deficient kidney, we treated kidney-targeted *Setd2* knockout mouse with a variety of inhibitors for SLC family transporters. Interestingly, increase in urine excretion after the administration of dapagliflozin, a SGLT2 inhibitor, was less in kidney-specific *Setd2* knockout mouse compared to control mouse, whereas increases in urine excretion after administrations of S3226, an inhibitor for NHE3 inhibitor, or furosemide, a potent inhibitor for NKCC2, did not show any significant difference between kidney-specific *Setd2* knockout mouse and control mouse (Fig. 4A). Additionally, increases in sodium and glucose excretions after the administration of dapagliflozin were less in kidney-specific *Setd2* knockout mouse compared to control mouse, further supporting that *Sglt2*-mediated water, sodium and glucose reabsorptions might be suppressed in *Setd2*-deficient kidney (Fig. 4B and C). Taken together, *SETD2* might regulates water, sodium and glucose reabsorptions in renal tubule through the modulation of expressions of SLC family transporters including *SGLT2*.

Discussion

In this study, we demonstrated that inactivation of *Setd2* in murine kidney leads to hypovolemia with dysregulated water, sodium and glucose reabsorptions in renal tubule. RNA sequencing of *Setd2*-deficient kidneys exhibited the downregulation of SLC family-mediated membranous transport pathway, suggesting that dysregulated SLC family transporters might lead to hypovolemia. In addition, dapagliflozin-induced diuresis and glucose excretion were attenuated in kidney-specific *Setd2* knockout mouse, further supporting that *SETD2* may regulate SLC family transporters including *SGLT2*.

Sodium glucose co-transporter 2 (SGLT2) inhibitors are a class of new effective antihyperglycemic agents which inhibits glucose reabsorption in the proximal tubule of the kidney [6]. In addition to its efficacy for diabetes mellitus, SGLT2 inhibitors have significant efficacies for heart failure and chronic kidney disease, resulting in decreased cardiovascular-related mortality [7–10]. Although numerous studies have highlighted the clinical benefit of SGLT2 inhibitor administration, a regulatory mechanism for *SGLT2* expression remains elusive; hepatocyte nuclear factor (HNF)1α regulates *SGLT2* expression by directly binding to the *SGLT2* 5′ flanking region; circ_000166 inhibits miR-296-dependent suppression of *SGLT2* expression; adiponectin from adipose tissue decreases *SGLT2* expression in renal tubule [11–13]. In this study, we demonstrated a new regulatory mechanism for *SGLT2*, which may provide a unique opportunity to further improve outcome of patients with diabetes mellitus, heart failure and chronic kidney disease.

Dysregulation of a crosstalk between metabolism and epigenome drives renal tumorigenesis, since most of renal tumor suppressors are associated with either metabolism or chromatin remodeling [14]. *SETD2*-deficient kidney cancer cell lines have been reported to exhibit an increased oxidative phosphorylation with upregulated *PGC1a* and its downstream genes [15]. In this study, inactivation of *Setd2* in murine kidney resulted in decreased expressions of SLC family transporters including *Sglt2*, which may lead to downregulated *Sglt2*-dependent glucose uptake and consequently trigger a metabolic shift toward oxidative phosphorylation in nephron cells, further suggesting that dysregulated metabolism may drive renal tumorigenesis in *SETD2*-deficient kidney cells.

The findings in this study illuminate an important role for *SETD2* in regulation of SLC family transporters-mediated sodium and glucose homeostasis. These data provide mechanistic insights into pathophysiology of diabetes mellitus, hypertension, cardiovascular disease and chronic kidney disease as well as further our understanding on renal tumorigenesis under *SETD2* deficiency, which may provide a unique opportunity to develop novel therapeutics and diagnostics for those diseases.

Material and Methods

Animals

All the animal experiments were performed in accordance with ARRIVE guidelines (https://arriveguidelines. org) under the approved protocols by the Institutional Animal Care and Use Committee at Yokohama City University. Mice were housed in the rodent barrier facility at Animal Center of Yokohama City University, at room temperature of 25°C and relative humidity of 50–60%, with a dark–

light cycle of 12 h, and had free access to food and water. Adult mice on a C57BL/6J background were anesthetized using isoflurane during experiments and euthanized using carbon dioxide in accordance with AVMA Guidelines for the Euthanasia of Animals: 2020 Edition. Mice carrying *Setd2* alleles flanked by loxP sites *(floxed, f)* were generated by Dr. Gang Huang at Cincinnati Children's Hospital Medical Center and kindly provided by Drs. Takashi Ishiuchi, Seiichi Yano and Hiroyuki Sasaki at Kyushu University, Fukuoka, Japan [2]. *Pax8-Cre* transgenic mice were purchased from Jackson Laboratory.

Genotyping

The following primers were used to detect floxed or wild-type alleles of *Setd2*: Fwd (5'-TTCTGGGAATCATCCATGGT-3') and Rev (5'-GAGCTCATTGTCAACACAAACAG – 3'). The *Setd2* floxed-allele was identified by the 1086-bp band and the wild-type allele was identified as a 1014-bp band. The following primers were used to detect *Pax8-Cre* allele: FwdI (5'-TCTCCACTCCAACATGTCTGC-3'), Fwd (5'-CCCTCCTAGTTGATTCAGCCC-3'), and Rev(5'-AGCTGGCCCAAATGTTGCTGG-3'). The *Pax8-Cre* allele was identified by the 500-bp band and the wild-type allele was identified as a 389-bp band.

Metabolic cage analysis and water restriction study

Mice with 10 weeks of age were acclimated to metabolic cages (Tecniplast, Italy) for the following week. After two additional days, daily body weight (BW), food intake, water intake and urine volume were measured. Mice were given free access to water and fed the standard diet. In water restriction study, urine was collected for twenty-four hours before and after water intake was restricted for twenty-four hours.

Blood pressure and heart rate measurements

Systolic blood pressure and heart rate were measured by the tail-cuff method (BP- monitor MK-2000; Muromachi Kikai Co., Japan). This system measures blood pressure in conscious mice without any preheating. Ten measurements were performed between 10AM and 2pm in each mouse.

Western Blotting

Tissues were homogenized in RIPA buffer supplemented with protease and phosphatase inhibitors. The protein concentration of each sample was measured using a TaKaRa BCA Protein Assay Kit (TaKaRa, Japan). Equal amounts of protein extract were fractionated on a 5–20% Mini-PROTEAN TGX precast gels (Bio-Rad). The gel was then transferred to a polyvinylidene difluoride (PVDF) membrane using a Wet/Tank Blotting Systems (Bio-Rad). Membranes were blocked for one hour at room temperature with blocking buffer (5% w/v BSA 1X TBS 0.1% Tween-20), and probed overnight at 4°C with a specific primary antibody. Membranes were washed and further incubated with secondary antibodies for one hour at room temperature. The sites of the antibody–antigen reaction were visualized by enhanced chemiluminescence substrate (GE Healthcare). Images were analyzed quantitatively using a Fuji LAS-3000 image analyzer (Fuji Film, Japan). Following antibodies were used: SETD2 (E4W8Q) Rabbit mAb (#80290), Tri-Methyl-Histone H3 (Lys36) (D5A7) XP® Rabbit mAb (#4909), Di-Methyl-Histone H3 (Lys36) (C75H12) Rabbit mAb (#2901), Histone H3 (D1H2) XP® Rabbit mAb (#4499), β-Actin Antibody (#4967) from Cell Signaling Technology.

Diuretic Test

A diuretic test was performed in a metabolic cage. One hour after intraperitoneal injection of 70 μL/g BW normal saline to facilitate spontaneous voiding, mice were intraperitoneally injected with 1 mg/mL dapagliflozin (Sigma-Aldrich) solution, 20 mg/mL S3226 (Sigma-Aldrich) solution, or 5 mg/mL furosemide (Sigma-Aldrich) solution in 10% DMSO at the volume of 10 μL/g BW. Urine was collected every hour by spontaneous voiding or bladder massage, and the urine volume and concentrations of sodium and glucose were measured.

RNA sequencing analysis

Total RNA was extracted using TRIzol (Thermo Fisher), RNeasy Mini kit (Qiagen) and RQ1 RNase-free DNase Set treatment (Promega). RNA sequencing (RNA-seq) was performed by Bioengineering Lab. Co., Ltd. (Japan). The libraries were generated using MGIEasy RNA Directional Library Prep Set (MGI Tech Co., Ltd.). Indexed samples were sequenced by DNBSEQ-G400 (MGI Tech Co., Ltd.). At least 20 million of 100-bp paired-end reads were acquired for each sample. Adaptors were trimmed using cutadapt (ver. 1.9.1). Reads with less than 20bp-length from Read 1 and those with less than 40bp-length from Read 2 were removed using sickle (ver 1.33). Reads were mapped to the Mus musculus reference genome GRcm39 (https://www.ncbi.nlm.nih.gov/assembly/GCF_000001635.27) using hisat2 (ver. 2.2.0). Read count was performed using featureCounts (ver. 2.0.0). Analysis of Differential Expressed Genes (DEG) was performed with edgeR (ver. 3.38.1). Reactome pathway analysis was performed with clusterProfiler (ver. 4.4.1).

Statistical analysis

All statistical analysis was performed with R (ver. 3.6.0) using Student's t test. All data are shown as the mean ± SEM and *p*-value less than 0.05 was considered to be statistically significant.

Declarations

Acknowledgements

We thank Ms. Hiromi Soeda and Mr. Takayuki Akagi in Department of Molecular Pathology, Yokohama City University for their excellent works in histological analyses.

Author Contributions

T.M., H.W., K.Azushima, K.T. and H.H. conceived the idea, designed the experiments and wrote the paper. T.M., T.U., R.J., S.O., G.N., S.K., Y.I., K.Aomori, K.N., A.N. and T.Kawagoe performed experiments. T.M., H.W., K.Azushima, T.U., T.Tatenuma., M.K., H.I., T.Kawahara, Y.I., K.Muraoka, M.F., I.K., S.F. T.Tamura, N.M., Y.K., H.U., M.Y., K.Makiyama. and H.H. analyzed the data. G.H. kindly provided *Setd2* floxed mice.

Data availability statement

RNA sequencing data were deposited under an accession number DRA016477 (ycumitome-0001_Submission), BioProject: PRJDB14815 (PSUB019056), BioSample: SAMD00565331-SAMD00565342 (SSUB023686) in DNA Data Bank of Japan (https://ddbj.nig.ac.jp/resource/sra-submission/DRA016477).

Declaration of interest

Authors were supported by JSPS KAKENHI Grant Number as following; H.H. by 23K08717, H.W. by 23K06871, K.Azushima. by 23K07678, H.I. by 20K18121, K.T. by 22K16821, M.Komeya. by 21H03068 22K19588, Y.I. by 19K18591, S.F. by 22K09730, K.N. by 21K06930, T.Tamura. by 21H02954, Y.K. by 23K08574.

References

1. Li, X. J. *et al.* Deficiency of Histone Methyltransferase SET Domain-Containing 2 in Liver Leads to Abnormal Lipid Metabolism and HCC. Hepatology 73, 1797–1815 (2021). https://doi.org/10.1002/hep.31594
2. Zhou, Y. *et al.* Setd2 regulates quiescence and differentiation of adult hematopoietic stem cells by restricting RNA polymerase II elongation. Haematologica 103, 1110–1123 (2018). https://doi.org/10.3324/haematol.2018.187708
3. Duns, G. *et al.* Histone methyltransferase gene SETD2 is a novel tumor suppressor gene in clear cell renal cell carcinoma. Cancer Res 70, 4287–4291 (2010). https://doi.org/10.1158/0008-5472.CAN-10-0120
4. Xie, Y. *et al.* SETD2 loss perturbs the kidney cancer epigenetic landscape to promote metastasis and engenders actionable dependencies on histone chaperone complexes. Nat Cancer 3, 188–202 (2022). https://doi.org/10.1038/s43018-021-00316-3
5. Rao, H. *et al.* Multilevel Regulation of beta-Catenin Activity by SETD2 Suppresses the Transition from Polycystic Kidney Disease to Clear Cell Renal Cell Carcinoma. Cancer Res 81, 3554–3567 (2021). https://doi.org/10.1158/0008-5472.CAN-20-3960
6. Augusto, G. A., Cassola, N., Dualib, P. M., Saconato, H. & Melnik, T. Sodium-glucose cotransporter-2 inhibitors for type 2 diabetes mellitus in adults: An overview of 46 systematic reviews. Diabetes Obes Metab 23, 2289–2302 (2021). https://doi.org/10.1111/dom.14470
7. Cowie, M. R. & Fisher, M. SGLT2 inhibitors: mechanisms of cardiovascular benefit beyond glycaemic control. Nat Rev Cardiol 17, 761–772 (2020). https://doi.org/10.1038/s41569-020-0406-8
8. Vallon, V. & Verma, S. Effects of SGLT2 Inhibitors on Kidney and Cardiovascular Function. Annu Rev Physiol 83, 503–528 (2021). https://doi.org/10.1146/annurev-physiol-031620-095920
9. Szekeres, Z., Toth, K. & Szabados, E. The Effects of SGLT2 Inhibitors on Lipid Metabolism. Metabolites 11 (2021). https://doi.org/10.3390/metabo11020087

10. van der Aart-van der Beek, A. B., de Boer, R. A. & Heerspink, H. J. L. Kidney and heart failure outcomes associated with SGLT2 inhibitor use. *Nat Rev Nephrol* 18, 294–306 (2022). https://doi.org/10.1038/s41581-022-00535-6
11. Chen, S. circ_000166/miR-296 Aggravates the Process of Diabetic Renal Fibrosis by Regulating the SGLT2 Signaling Pathway in Renal Tubular Epithelial Cells. *Dis Markers* 2022, 6103086 (2022). https://doi.org/10.1155/2022/6103086
12. Pontoglio, M. *et al.* HNF1alpha controls renal glucose reabsorption in mouse and man. EMBO Rep 1, 359–365 (2000). https://doi.org/10.1093/embo-reports/kvd071
13. Zhao, Y. *et al.* Sodium Intake Regulates Glucose Homeostasis through the PPARdelta/Adiponectin-Mediated SGLT2 Pathway. Cell Metab 23, 699–711 (2016). https://doi.org/10.1016/j.cmet.2016.02.019
14. Hasumi, H. & Yao, M. Hereditary kidney cancer syndromes: Genetic disorders driven by alterations in metabolism and epigenome regulation. Cancer Sci 109, 581–586 (2018). https://doi.org/10.1111/cas.13503
15. Liu, J. *et al.* Loss of SETD2 Induces a Metabolic Switch in Renal Cell Carcinoma Cell Lines toward Enhanced Oxidative Phosphorylation. J Proteome Res 18, 331–340 (2019). https://doi.org/10.1021/acs.jproteome.8b00628

Figures

Figure 1

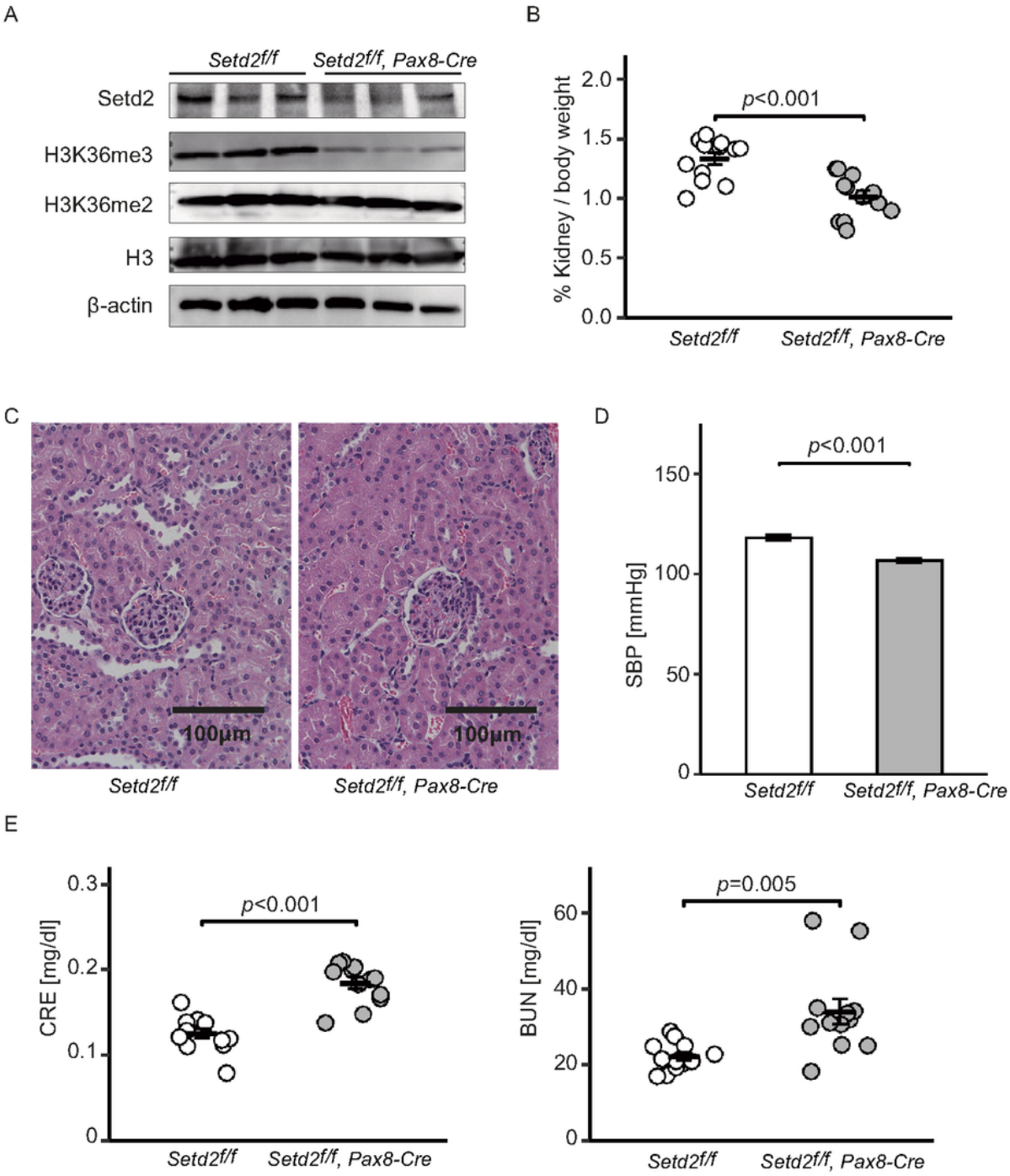

Figure 1

Kidney-specific inactivation of *Setd2* leads to hypovolemia with renal dysfunction in mouse.

(A) Conditional *Setd2* knockout mice were crossbred with *Pax8-Cre* transgenic mice. Western blotting shows inactivation of *Setd2* and decrease in H3K36me3 protein in *Setd2*-deficient kidneys. n=3 each at 10 weeks of age.

(B) Kidney weight per body weight ratio was decreased in kidney-specific *Setd2*knockout mice. n=12 each at 10 weeks of age. Mean+SEM. Student *t*-test.

(C) Representative H&E staining of control and *Setd2*-deficient kidneys at 10 weeks of age did not show any histological difference.

(D) Systolic blood pressure (SBP) was decreased in kidney-specific *Setd2* knockout mice. n=7 each at 10 weeks of age. Mean+SEM. Student *t*-test.

(E) Plasma creatinine (CRE) and blood urea nitrogen (BUN) were increased in kidney-specific *Setd2* knockout mice. n=12 each at 10 weeks of age. Mean+SEM. Student *t*-test.

Figure 2

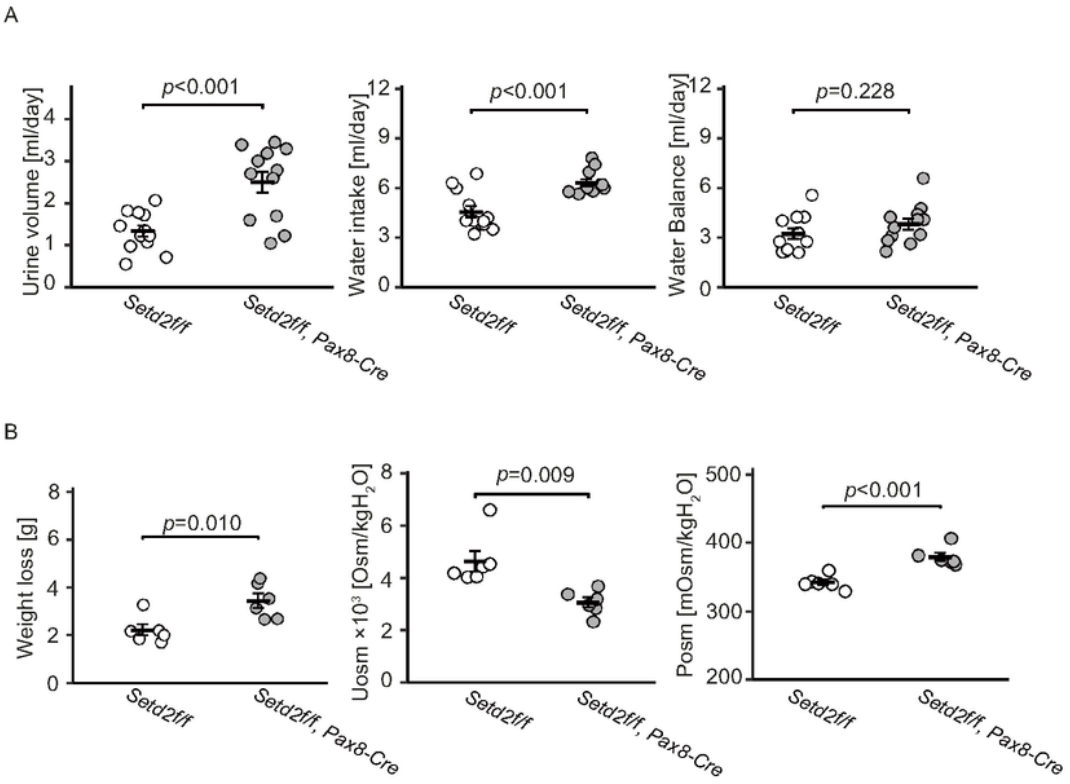

Figure 2

Kidney-specific inactivation of *Setd2* leads to defective urinary concertation in mouse.

(A) Urine volume, water intake and water balance per day were measured using metabolic cage. n = 12 each at 10 weeks of age. Mean+SEM. Student *t*-test.

(B) Body weight loss, urine osmolality (Uosm) and plasma osmolality (Psom) were measured after water restriction for 24 hours. n = 6 each at 10 weeks of age. Mean+SEM. Student *t*-test.

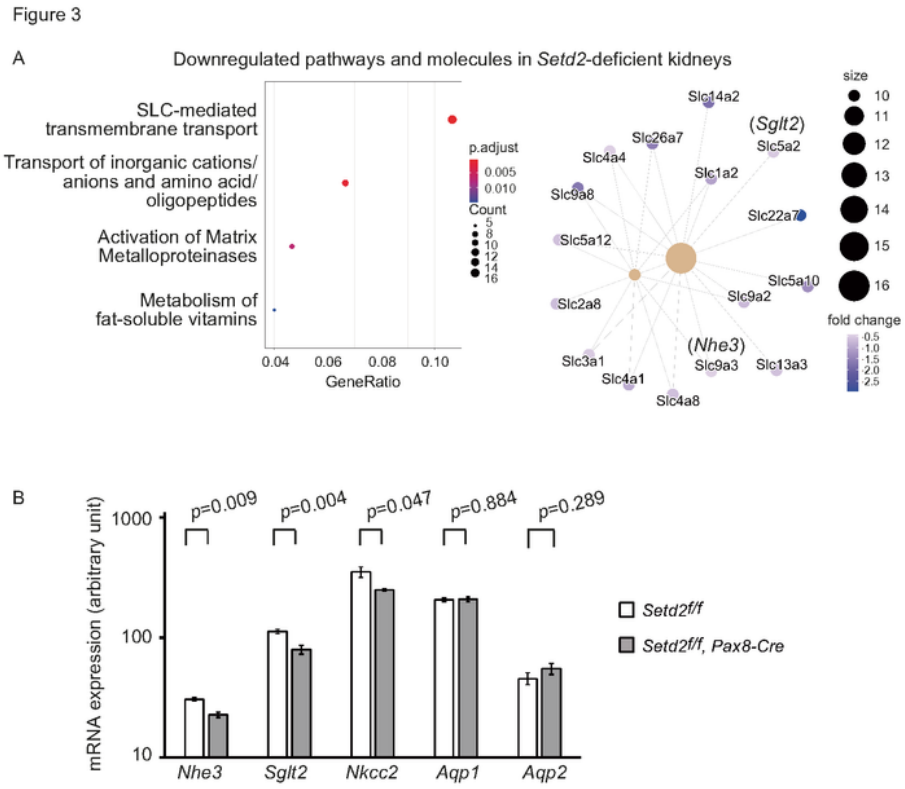

Figure 3

Kidney-specific inactivation of *Setd2* leads to decreased expressions of SLC family transporters.

(A) Reactome pathway analysis was done using RNA-seq data of control and *Setd2*-deficient kidneys. Downregulated pathways in *Setd2*-deficient kidneys are shown in the left panel. Cnet plots for “SLC-mediated transmembrane transport” and “Transport of inorganic cations/anions and amino acid/oligopeptides” are shown in the right panel. n = 6 each at 10 weeks of age.

(B) Expressions of SLC family transporters are shown from RNA-seq data of control and *Setd2*-deficient kidneys. n = 6 each at 10 weeks of age. Mean+SEM. Student *t*-test.

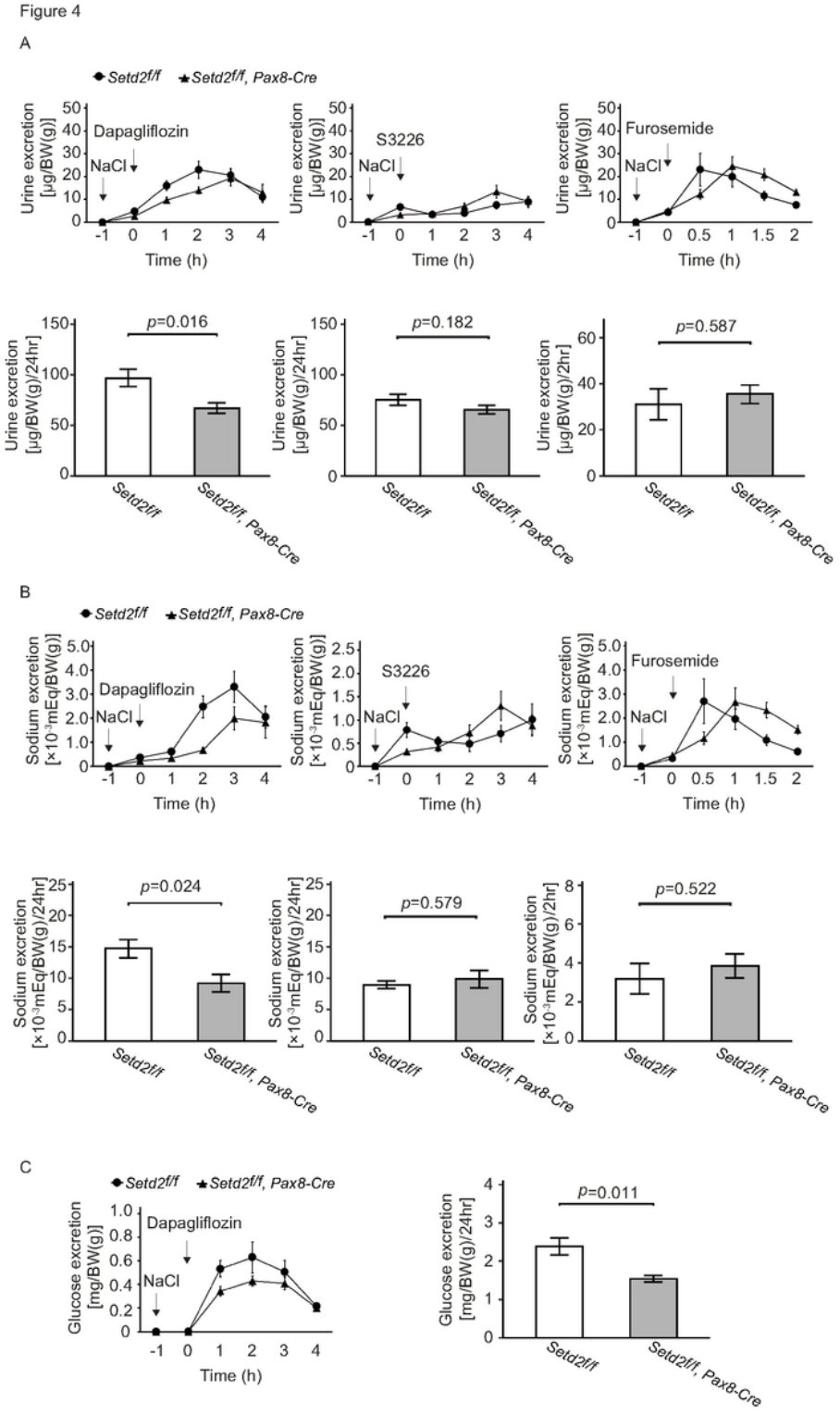

Figure 4

***Setd2*-deficient kidney exhibits attenuated dapagliflozin-induced diuresis and glucose excretion.**

(A) Line plots show urine excretions after administrations of dapagliflozin, S3226 or furosemide. Urine excretions per day after dapagliflozin and S3226 administrations, and urine excretions for two hours after furosemide administration are shown in the lower panels. n=6 each at 10 weeks of age. Mean+SEM. Student *t*-test.

(B) Line plots show urinary sodium excretions after administrations of dapagliflozin, S3226 or furosemide. Urinary sodium excretions per day after dapagliflozin and S3226 administrations, and urinary sodium excretions for two hours after furosemide administration is shown in the lower panels. n=6 each at 10 weeks of age. Mean+SEM. Student *t*-test.

(C) Line plots show urinary glucose excretions after dapagliflozin administration. Urinary glucose excretions per day are shown in the right panel. n=6 each at 10 weeks of age. Mean+SEM. Student *t*-test.

Supplementary Files

This is a list of supplementary files associated with this preprint. Click to download.

- SupplementaryFigure.pdf